Effects of the impurity–host interactions on the nonradiative processes in ZnS:Cr

C. Tablero[a)]
Instituto de Energía Solar, Universidad Politécnica de Madrid, Ciudad Universitaria s/n, 28040 Madrid, Spain

(Received 29 July 2010; accepted 28 September 2010; published online xx xx xxxx)

There is a great deal of controversy about whether the behavior of an intermediate band in the gap of semiconductors is similar or not to the deep-gap levels. It can have significant consequences, for example, on the nonradiative recombination. In order to analyze the behavior of an intermediate band, we have considered the effect of the inward and outward displacements corresponding to breathing and longitudinal modes of Cr-doped ZnS and on the charge density for different processes involved in the nonradiative recombination using first-principles. This metal-doped zinc chalcogenide has a partially filled band within the host semiconductor gap. In contrast to the properties exhibited by deep-gap levels in other systems, we find small variations in the equilibrium configurations, forces, and electronic density around the Cr when the nonradiative recombination mechanisms modify the intermediate band charge. The charge density around the impurity is equilibrated in response to the perturbations in the equilibrium nuclear configuration and the charge of the intermediate band. The equilibration follows a Le Chatelier principle through the modification of the contribution from the impurity to the intermediate band and to the valence band. The intermediate band introduced by Cr in ZnS for the concentrations analyzed makes the electronic capture difficult and later multiphonon emission in the charge-transfer processes, in accordance with experimental results.

I. INTRODUCTION

There is a great deal of interest in developing new semiconductor materials with a high concentration of electronic levels within the semiconductor band gap. Interest in this subject has been revitalized by the observation of a wide variety of magnetic and optical properties shown by these systems in heavily doped samples. These doped materials can have an intermediate band (IB) between the valence band (VB) and the conduction band (CB) of the host semiconductor which, in a formal band-theoretic picture, can be metallic if the Fermi energy lies within the impurity band. This basic electronic band structure corresponds to a class of materials, known as IB materials, and is characteristic of transparent conducting oxides, certain types of up- and down-converters, some spintronic devices, midinfrared lasers and IB solar cells.[1] Focusing on solar cells, the presence of the IB allows photons of lower energy than the gap to be absorbed, promoting electrons from the VB to the IB, thus generating holes in the VB, and from the IB to the CB, generating electrons in the CB. In addition to this process of carrier generation, the usual process of generation by photon absorption, promoting electrons from the VB to the CB, also takes place. The number of carriers (electrons in the CB and holes in the VB) generated when there is an IB is greater than when there is not, because of the additional VB–IB and IB–CB transitions. Therefore, the presence of the IB would increase the efficiency of solar cells, provided no voltage loss compensates for the current gain.[1] For this process to take place, it is necessary for the IB to be partially filled, with both empty states to accommodate electrons from the VB–IB transition, and occupied states to provide electrons for the IB–CB transition. These materials have been studied in some detail during recent years.[2]

However, there is a great deal of controversy about whether the IB increases the nonradiative recombination (NRR) in a similar form to the deep gap levels in semiconductors. Although the nonradiative transitions are very important, their nature is rarely analyzed in detail since their consequences are usually only seen negatively for optoelectronic applications. Among the NRR mechanisms, one of the most important related to the charge-transfer processes is the mechanism via multiphonon emission (MPE).[3] This mechanism is illustrated in Fig. 1.

In this figure, the energy curves of the $D^{\alpha}+e_{\mathrm{VB}}$, $D^{\alpha+1}$, and $D^{\alpha}+e_{\mathrm{CB}}$ systems are represented with respect to the configuration coordinate Q. D^{α} indicates the impurity electronic configuration. e_{VB} and e_{CB} represent an electron in the VB and CB, respectively. The crossing point Q_C is the generalized coordinate where the electronic energy of the systems $D^{\alpha}+e_{\mathrm{CB}}$ and $D^{\alpha+1}$ is equal. Similarly, the $D^{\alpha}+e_{\mathrm{VB}}$ and $D^{\alpha+1}$ energy curves cross in the generalized coordinate Q_V. The thermal energies $E_t^{(i)}$ are the energies between equilibrium configurations and involve the strain energy of the distortion as well as a purely electronic part. The optical energies $E_o^{(i)} = E_t^{(i)} + E_r^{(i)}$ correspond to vertical transition with equal Q, where $E_r^{(i)}$ are the relaxing energies. These energies are directly related to the difference between the equilibrium configurations and force constants of the states involved.[3,4] The energy difference between optical absorption and optical emission is known as the Stokes shift. Such a shift between

a)Electronic mail: ctablero@etsit.upm.es.

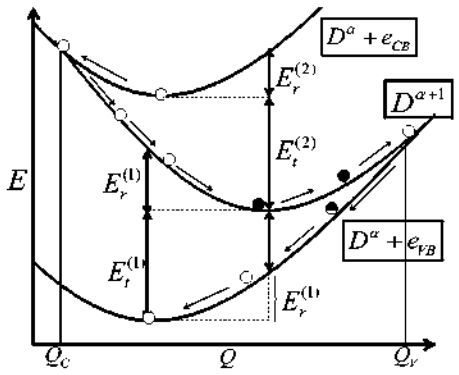

FIG. 1. (Color online) Schematic representation of the MPE-NRR mechanism. The energy curves represent the energy of the $D^{\alpha}+e_{VB}$, $D^{\alpha+1}$, and $D^{\alpha}+e_{CB}$ systems with respect to the configuration coordinate Q. e_{VB} and e_{CB} represents an electron in the VB and CB, respectively. Q_V is the crossing point of the energy curves corresponding to the systems $D^{\alpha}+e_{VB}$ and $D^{\alpha+1}$. Similarly, Q_C is the crossing point of the $D^{\alpha}+e_{CB}$ and $D^{\alpha+1}$ energy curves.

absorption and luminescent energies is well known in luminescent materials. The Stokes shift is related with the Frank–Condon shift $E_{FC}^{(i)}$ and the Huang–Rhys factor S_i. When all modes have the same frequency ω_i and the energy is a quadratic function of the configuration coordinate Q, then $E_{abs}^{(i)}-E_{emi}^{(i)}=2E_{FC}^{(i)}=2E_r^{(i)}=2S_i\hbar\omega_i$. For the nonradiative capture enough energy to reach the cross-over is required. Therefore, the relaxing energies represent the activation energy for the nonradiative capture. Obviously, the NNR is inhibited when the two curves involved in the nonradiative transition do not cross, or when the crossing point correspond to very high energies with respect to the equilibrium configurations. This happens when the energy curves involved in the nonradiative transition are *parallels*, i.e., the equilibrium configurations and force constants of the two energy curves are similar.

The MPE mechanism takes place when an impurity deep level is present. It occurs basically in two capture steps (Fig. 1). An electron in the CB (e_{CB}) is first captured around Q_C in an impurity state ($D^{\alpha}+e_{CB}\rightarrow D^{\alpha+1}$) and then the electron recombines with a hole in the VB around Q_V (hole capture $D^{\alpha+1}+h_{VB}\rightarrow D^{\alpha}$ or $D^{\alpha+1}\rightarrow D^{\alpha}+e_{VB}$, where h_{VB} represents a hole in the VB). After the transitions (captures), there is a large modification of the electronic density around the impurity, and as a consequence, the forces on the impurity will be significant. These forces cause a modification in the position of the impurity. They can be classified in terms of the mean distortions on the equilibrium positions of the $D^{\alpha}+e_{CB}$, $D^{\alpha+1}$, and $D^{\alpha}+e_{VB}$ energy curves, directly related to the Huang–Rhys factor or the Frank–Condon shift.[3] The large vibrational energy, which is initially localized at the impurity center, will propagate away from the center in the form of lattice phonons. This mechanism of recombination gives rise to violent, short-lived lattice vibrations localized at the defect which greatly enhance the probability of defect motion.

Therefore, in order to diminish the NRR, the impurity charge changes with Q for the $D^{\alpha}+e_{CB}\rightarrow D^{\alpha+1}$ and $D^{\alpha+1}\rightarrow D^{\alpha}+e_{VB}$ processes should be small. Then the energy curves of $D^{\alpha}+e_{VB}$, $D^{\alpha+1}$, and $D^{\alpha}+e_{CB}$ will be almost *parallel*. These charges added to or removed from the impurity should be redistributed in order to have an almost constant impurity charge density. There are following two forms: redistribution between all the impurities and redistribution with the host semiconductor. The former was related to the Mott transition.[4,5] In this work, we analyze the later mechanism. Anyway, there would be a small variation in the electronic density around the impurity atom. Then, in a configuration coordinate diagram, the equilibrium positions of the $D^{\alpha}+e_{CB}$, $D^{\alpha+1}$, and $D^{\alpha}+e_{VB}$ energy curves would be almost the same and the crossing points Q_C and Q_V will be at very high energies. This point is very important for comparing the NRR of a system with an IB, resulting in the combination of the host and the impurity orbitals, with respect to impurity deep-gap levels in other systems with lower impurity concentration. From now, and in the following sections, our goal will be the confirmation of this fact.

From all of the aforementioned, there are two main factors that influence the MPE mechanism related with the impurity charge modification as follows: (i) the change with respect to the electrons added to or removed from the impurity+host system, and (ii) the alteration with the generalized coordinate Q. In this work, we will analyze these two main factors.

To carry it out, we will examine a material derived from the ZnS host semiconductor where the Cr is incorporated uniformly by substituting the host metallic atom (one Cr for one of the 32 Zn atoms, i.e., $Zn_{1-x}Cr_xS$ with $x=1/32$). The reason for choosing this system is that the absorption and emission properties of similar transition-metal-doped zinc chalcogenides have been researched in order to understand their potential application as room temperature, midinfrared tunable laser media.[6] Room-temperature lasing has been demonstrated for the Cr doped crystals of ZnS and ZnSe. From these results, highly favorable lasers for the midinfrared are produced when Cr is a dopant in the zinc chalcogenides because only the Cr appears to be significantly free of the negative effects of nonradiative decay. On the other hand, theoretical studies on transition-metal-doped zinc chalcogenides[7] show that the doping with Cr is the transition-metal-doped zinc chalcogenide which shows the presence of a partially full IB more clearly.

Another reason for choosing this system is that the correlation effects have been analyzed intensively. Because of the IB characteristics, narrow compared with the gap of the host semiconductor and partially filled, correlation effects could be very important. In reference,[7] two possible mechanisms that would split the IB into two subbands, a full one and an empty one, i.e., metal–insulator transition, have been analyzed; a Jahn–Teller distortion and the correlation effects. None of these mechanisms leads to a metal–insulator transition.

II. CALCULATIONS

One useful approach to obtain and understand the electronic properties is from density functional method (DFT) (Ref. 8) with the local spin density approximation (LSDA). As is well-known, single-particle LSDA levels have no rigorous meaning. We thus calculate the energy curves involved in the NRR mechanism using total energies.

When the impurity takes up a substitutional site in the host semiconductor, the impurity+host system is neutral, its total energy is $E[0;D^{\alpha}]$, and the formal configuration of the impurity is D^{α}. If n electrons are removed, the total charge is n, its total energy is $E[n;D^{\alpha-n}]$, and the formal configuration of the impurity is $D^{\alpha-n}$. The formation energy of the multiply charged impurity+host system is defined as

$$\Delta H(E_F,n) = E(n;D^{\alpha-n}) - E_H(0) - \sum_i n_i\mu_i + nE_F$$

$$= E(n;D^{\alpha-n}) - E(0;D^{\alpha}) + nE_F, \quad (1)$$

where E_F is the Fermi energy, $E_H(0)$ is the total energy for the neutral solid containing only host atoms, n_i indicates the number of atoms of type i (host atoms or impurity atoms) that have been added to ($n_i>0$) or removed from ($n_i<0$) the solid when the defect or impurity is created, and the μ_i are the corresponding chemical potentials of these species. These chemical potentials represent the energy of the reservoirs with which atoms are being exchanged.

The energy implicated in the recombination processes $D^{\alpha}+e_{CB}\rightarrow D^{\alpha+1}$ and $D^{\alpha+1}\rightarrow D^{\alpha}+e_{VB}$ are $\varepsilon_{\alpha+1}-\varepsilon_{CB}$ and $\varepsilon_{VB}-\varepsilon_{\alpha+1}$, respectively, where $\varepsilon_{\alpha+1}\equiv\varepsilon_A$ is the acceptor ionization energy. These ionization energies correspond to the value of the Fermi energy at which the impurity or the defect changes from a charge state α to $\alpha\pm1$.[9] These energies correspond to the solution of $\Delta H(\varepsilon_{\alpha},0)=\Delta H(\varepsilon_{\alpha},1)$ and $\Delta H(\varepsilon_{\alpha+1},0)=\Delta H(\varepsilon_{\alpha+1},-1)$. Therefore, the acceptor $\varepsilon_{\alpha+1}\equiv\varepsilon_A$ and donor $\varepsilon_{\alpha}\equiv\varepsilon_D$ ionization energies can be obtained from total energy calculations as $\varepsilon_{\alpha}=E(0;D^{\alpha})-E(1;D^{\alpha-1})$ and $\varepsilon_{\alpha+1}=E(-1;D^{\alpha+1})-E(0;D^{\alpha})$. The previous equations give the absolute energy levels. However, they are usually referred to the bottom of the CB ($\varepsilon_{\alpha}^{(CB)}=\varepsilon_{CB}-\varepsilon_{\alpha}$) or to the top of the VB ($\varepsilon_{\alpha+1}^{(VB)}=\varepsilon_{\alpha+1}-\varepsilon_{VB}$). $\varepsilon_{\alpha}^{(CB)}$ and $\varepsilon_{\alpha+1}^{(VB)}$ represent the donor and acceptor ionization energies corresponding to the processes $D^{\alpha}\rightarrow D^{\alpha-1}+e_{CB}$ and $D^{\alpha}+e_{VB}\rightarrow D^{\alpha+1}$, respectively.

To find a coherent description of both defect energies and the band edge energies, we obtain them both from electron addition and removal calculations, i.e., in a similar way to the energy levels using the Eq. (1) with all μ_i zero; $\Delta H_H(E_F,n)=E_H(n)-E_H(0)+nE_F$, where $E_H(n)$ is the ground state energy of the defect-free supercell as a function of the charge n in it. Note that the conduction and VB edge energies are the acceptor (electron affinity $\varepsilon_{CB}=[E_H(-1)-E_H(0)]$) and donor (ionization energy $\varepsilon_{VB}=[E_H(0)-E_H(+1)]$) energies for the host system. The band gap obtained from total energy calculations ($\varepsilon_{CB}-\varepsilon_{VB}=[E_H(-1)-2E_H(0)+E_H(+1)]$) is much closer to the experimental than the calculated from single-particle Kohn–Sham eigenvalues.

The nomenclature used here is borrowed historically from the field of the ionic compounds where the charge transfer is almost complete. In solids and molecules, to speak of the configurations is inadequate because the impurity-host or atom–atom bonding is in general not ionic with a total charge transfer. We will use it here as a formal notation.

In order to obtain the total energies $E(-1;D^{\alpha+1})$, $E(0;D^{\alpha})$, $E(+1;D^{\alpha+1})$, $E_H(-1)$, $E_H(0)$, and $E_H(+1)$, need to calculate the ε_A, ε_D, ε_{VB}, and ε_{CB} energies, we use the DFT with pseudopotentials[10] for core electrons and numerically localized pseudoatomic orbitals[11] as the basis set for the valence wave functions. The LSDA as proposed by Ceperley–Alder[12] for the exchange and correlation term is used. We use periodic boundary conditions with 18 special k points in the irreducible Brillouin zone. In all calculations, a double-zeta with polarization functions basis set has been used. The atom positions of the supercell are allowed to relax according to the calculated quantum mechanical forces (with no symmetry constraints) until the total energy minimum was reached and the forces became less than 0.004 eV/Å. The supercell approach is also used to simulate different charge states of the impurity. The energy of a periodically repeated electrically charged system diverges, and thus a jellium background is adopted to neutralize the charge. In these cases electrons are removed from (added to) the supercell to (from) a noninteracting reservoir, where they do not contribute to the exchange-correlation or Hartree potential, except through the zero-Fourier component of the charge density. In other words, a rigid background charge density smeared out over the entire cell is introduced in order to neutralize the supercell.

III. RESULTS

Firstly, all atomic positions in the supercell of the impurity+host system have been relaxed without symmetry constrains. The results show a C_{3v} symmetry distortion around the Cr atom; one Cr–S bond length is 2.62 Å and three lengths are 2.50 Å. Therefore, there are two nonequivalent groups of S atoms around the Cr atom, labeled as S_1 and S_3; one S_1 and three S_3 atoms. Because of the approximately tetrahedral symmetry, the d-Cr orbitals split in to groups, the t-Cr (d_{xy}, d_{xz}, and d_{yz}) and e-Cr (d_{z^2} and $d_{x^2-y^2}$) orbitals. In addition, the spin interaction splits these two groups into four as follows: e_+-Cr and t_+-Cr for majority spin, and e_--Cr and t_--Cr for minority spin.

The band structure presents a partially filled IB (Ref. 7) in the energy gap with two electrons per cell. This IB is the antibonding mix (larger energy) of the t_+-Cr and the t_+-anion orbitals around the Cr atom; $t_+\equiv IB(t_+)\approx a(t_+\text{-Cr})+b(t_+\text{-S})$. The bonding combination (lower energy) is within the VB [$VB(t_+)\approx c(t_+\text{-Cr})+d(t_+\text{-S})$]. The degree of combination of the atomic states in order to make up the bands depends on the total charge of the IB and on the generalized coordinate Q. The neutral system has a $t_+^2=D^2$ electronic configuration. Really it has an $e_+^2t_+^2$ configuration but e_+^2 is omitted for simplicity. This configuration corresponds with $Cr^{+2}(d^4)$. When one electron is added ($n=-1$) the IB is full [$t_+^3=D^3$ electronic configuration, which correspond with $Cr^{+1}(d^5)$], and when one electron is removed ($n=+1$) the IB is 1/3 occupied [$t_+^1=D^1$ electronic configuration, i.e., $Cr^{+3}(d^3)$].

In order to study the MPE mechanism we have considered several degrees of freedom in our calculations as follows: the symmetric (from ideal lattice sites) and nonsymmetric (from relaxed lattice sites) inward or outward displacement of the nearest neighbors of the Cr atom, i.e., breathing-modes (BMs), and the symmetric and nonsymmetric longitudinal modes (LMs), where the S atom in the (111)

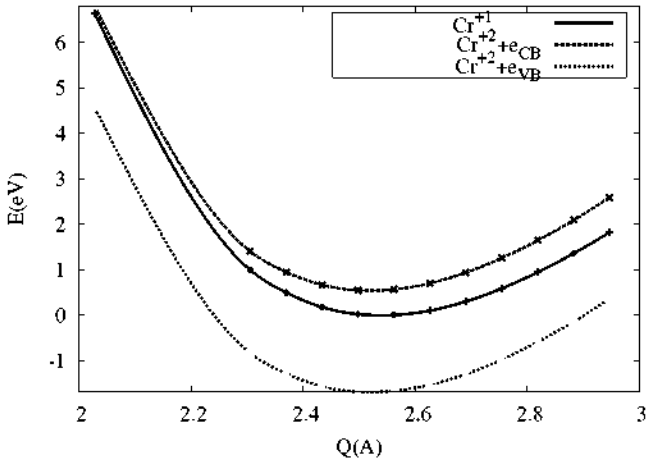

FIG. 2. (Color online) Configuration coordinate diagram in upward order of energy for $Cr^{+2}(d^4)+e_{VB}$, $Cr^{+1}(d^5)$, and $Cr^{+2}(d^4)+e_{CB}$. The total energy for the $Cr^{+1}(d^5)$ at the equilibrium configuration of the BM has been chosen as zero in this figure. Marks indicate the calculated structures and lines correspond to fits to these points.

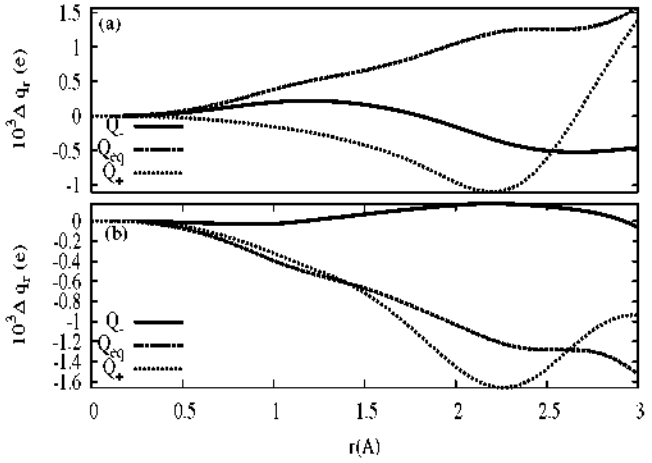

FIG. 3. (Color online) Difference (Δq_r) between Cr radial charge (electron charge units) as a function of the radius r (Å) of the sphere centered at the Cr position for $Cr^{+2}(d^4)+e_{CB}$ and $Cr^{+1}(d^5)$ (a), and $Cr^{+1}(d^5)$ and $Cr^{+2}(d^4)+e_{VB}$ systems (b). Δq_r is shown for three Q values: Q_{eq}, Q_+, and Q_-.

direction is displaced. In the BM (LM) all other atoms are kept at their ideal (symmetric) or relaxed (nonsymmetric) lattice sites, except the nearest four neighboring S atoms [the S atom in the direction (111)] of the Cr atom. For the nonsymmetric BM the Cr–S distances are scaled by an equal factor β, and we chose $Q=\beta\times(2.50$ Å) as a generalized coordinate. In the following we will focus on the more general nonsymmetric BM. The conclusions derived for the other modes are similar.

A. Energy curves

Because of the amphoteric character of Cr in ZnS, i.e., the impurity is both a donor and an acceptor (both donor and acceptor energies are in the gap), two processes take place $Cr^{+2}+e_{VB}\rightarrow Cr^{+}$ and $Cr^{+}\rightarrow Cr^{+2}+e_{CB}$ (direct and inverse sense corresponds to generation and recombination processes, respectively). The number of electrons and holes thermally released or light-induced to the CB and VB can be monitored by observing the changes in the intensity of the electron-paramagnetic-resonance signal.

In Fig. 2, the configuration coordinate diagram obtained from total energy calculations for the $Cr^{+2}(d^4)+e_{VB}$, $Cr^{+1}(d^5)$, and $Cr^{+2}(d^4)+e_{CB}$ in ZnS is shown. From Fig. 2, 2.10 and 0.93 eV are obtained for the electronic transitions $Cr^{+2}(d^4)+e_{VB}\rightarrow Cr^{+1}(d^5)$ and $Cr^{+1}(d^5)\rightarrow Cr^{+2}(d^4)+e_{CB}$. However, even when using total energy calculations, the ZnS gap is 0.8 eV lower than the experimental (3.84 eV). If the bands are shifting 0.4 eV each one to accommodate this discrepancy, these values are 2.50 and 1.33 eV, very close to the experimental ones [2.41 and 1.43 eV (Refs. 13 and 14)].

The experimental difference between thermal (transition between equilibrium configurations) and optical (vertical transition with equal Q) levels is 0.37 eV. This energy is directly related to the different lattice equilibrium positions for the charge states of the Cr. Our results show a lower relaxing energy. From Fig. 2 the minimums of the curves $Cr^{+2}(d^4)+e_{VB}$, $Cr^{+1}(d^5)$, and $Cr^{+2}(d^4)+e_{CB}$ are very similar. Therefore the Huang–Rhys factor and the Frank–Condon shift are very small. One reason for these relaxing energy discrepancies is the larger Cr concentration with respect to experimental results. Another reason is directly related to the Cr-S interaction in the IB and the VB: there are only small variations in the electronic density and forces around the Cr atom when the charge is modified in the recombination processes. This aspect will be analyzed next.

B. Charge density analyses

In order to confirm the previous results, we will carry out an analysis of the radial charge around the Cr atom $q_S(r)=\int_{|\mathbf{R}|\le r}d\mathbf{R}\rho_S(\mathbf{R})$. The radial charge is the charge in a sphere of radius r centered on the Cr atom, where ρ_S is the charge density of the system S. The increments in the radial charge around the Cr atom are shown in Fig. 3. For the process $Cr^{+2}(d^4)+e_{CB}\rightarrow Cr^{+1}(d^5)$ (panel a), Δq_r is the difference between Cr radial charge for $Cr^{+2}(d^4)+e_{CB}$ and $Cr^{+1}(d^5)$ systems. Similarly, in the panel b Δq_r is the difference between Cr radial charge for $Cr^{+1}(d^5)$ and $Cr^{+2}(d^4)+e_{VB}$ systems. Δq_r is shown for three Q values; Q_{eq}, a configuration larger than Q_{eq} ($Q_+>Q_{eq}$), and another lower than Q_{eq} ($Q_-<Q_{eq}$). The numerical values of Q_+, Q_{eq}, and Q_+ are, respectively, 1.87 Å, 2.50 Å, and 3.05 Å.

From the figure, the variations in the Cr radial charge within a sphere of radius 2.50 Å is less than 1.65×10^{-3} electrons for the two processes involved in the NNR. It is in accordance with the previous results on the energy curves; as a consequence of small variations in the electronic charge and density around the Cr atom with Q, the curves involved in the $D^{\alpha}+e_{CB}\rightarrow D^{\alpha+1}$ and $D^{\alpha+1}\rightarrow D^{\alpha}+e_{VB}$ processes do not cross, except at very high energies. Therefore, the positions of the minima of the curves will be similar, decreasing the Huang–Rhys factor or the Frank–Condon shift. This impedes the NRR.

The following step is to analyze the reason for this behavior. To do so we are going to study the contribution of the t_+-Cr states to the IB and the VB as an energy function for the processes in Fig. 1.

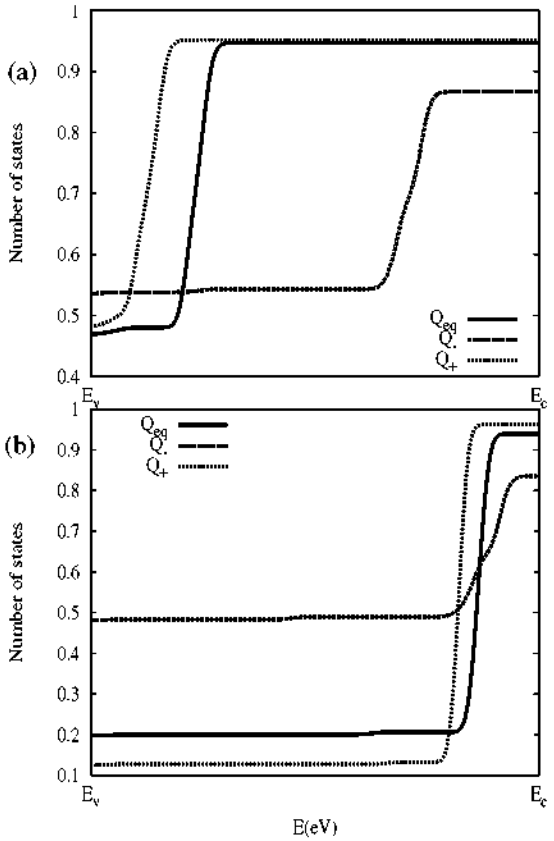

FIG. 4. (Color online) Number of t_+-Cr states as a function of the energy for t_+^2 (a) and t_+^3 (b) IB configurations for three configuration coordinates: at the equilibrium (Q_{eq}), a coordinate greater than Q_{eq} ($Q_+ > Q_{eq}$) and a coordinate smaller than Q_{eq} ($Q_- < Q_{eq}$). The Fermi energy as zero of the t_+^2 IB configuration at Q_{eq} has been chosen in this figure.

C. Analysis of the Cr contribution to the bands

The IB is the antibonding mix (larger energy) of the t_+-Cr and the t_+-anion orbitals; $t_+ \equiv \mathrm{IB}(t_+) \approx a(t_+\text{-Cr}) + b(t_+\text{-S})$, whereas the bonding combination (lower energy) is within the VB [$\mathrm{VB}(t_+) \approx c(t_+\text{-Cr}) + d(t_+\text{-S})$]. Obviously, when the IB charge is modified as a consequence of the NNR processes, a fraction is assumed by the Cr atom. From the results in previous section is fraction is small. The other portion is assumed by the S atoms directly connected with the Cr atom. For an impurity without strong interactions with the host atoms almost all charge of the IB (in this case it will a deep level, not a band) will correspond to the impurity because the larger contribution of the deep level will be from the impurity.

The following objective is to analyze how the t_+-Cr charge is modified as a consequence of the change in the IB charge. Figure 4 shows the number of t_+-Cr states as a function of the energy for $t_+^2 = D^2 = \mathrm{Cr}^{+2}$ (panel a) and $t_+^3 = D^3 = \mathrm{Cr}^+$ (panel b) IB configurations for three Q values; Q_{eq}, Q_+, and Q_-. In the energy axis, the edges of VB and CB are also shown. In a flat zone there are no contributions of the t_+-Cr orbitals. It can be a gap or simply that these orbitals do not contribute to this energy range. The contribution of the t_+-Cr states to the VB is the number of states for E_V (edge of the VB). The contribution to the IB is the difference between the number of states for E_C (edge of the CB) and E_V, or between the maximum and minimum of the IB. From the two panels in the figure, it is seen that in the gap there is a larger increment in t_+-Cr states corresponding to the IB.

A rise in the occupation of the IB (from t_+^2 to t_+^3, i.e., from panel a to b) has, as an effect, an increase in the contribution of the t_+-Cr states to the IB, but a decrease to the VB. Therefore, the effects of the modifications of the IB charge on the t_+-Cr are twofold; (1) an increment in the Cr atom charge because of the increase in the Cr contribution to the IB; (2) a decrease in the Cr atom charge because of a reduction in the Cr contribution to the VB. This behavior, first envisioned by Haldane and Anderson,[15] leads to small increase in the t_+-Cr charge (Δt_+-Cr) because of the charge increments in the VB ($\Delta t_+^{(\mathrm{VB})}$-Cr) and the IB ($\Delta t_+^{(\mathrm{IB})}$-Cr) are opposed: $[\Delta t_+\text{-Cr}] = [\Delta t_+^{(\mathrm{VB})}\text{-Cr}] + [\Delta t_+^{(\mathrm{IB})}\text{-Cr}] \approx 0$. The total charge on the Cr atom has a similar behavior. Therefore, contrary to what happens with isolated and deep impurities in semiconductors, the charge modification of the IB because of the NRR processes almost do not modify the Cr charge.

Additionally, in Fig. 4 it is observed that a decrease in Q has, as a consequence, a larger contribution of t_+-Cr states to the VB, but a lower contribution to the IB. Therefore, an increase in the impurity–host interaction with respect to the equilibrium configuration ($Q < Q_{eq}$) decreases (increases) the t_+-Cr impurity contribution to the IB (VB). In a similar way to what happened with the variation in the occupation of the IB, $[\Delta t_+\text{-Cr}] \approx 0$ because $[\Delta t_+^{(\mathrm{VB})}\text{-Cr}]$ and $[\Delta t_+^{(\mathrm{IB})}\text{-Cr}]$ are opposed. For the LM the results are similar, although the increments in the charges are lower than for the BM.

IV. DISCUSSION

Based on the calculated results, when a charge is added to or eliminated from the IB, it will be distributed between the d-Cr and the host orbitals. This behavior of the impurity contribution to the IB and VB with respect to the IB occupation and the interaction impurity–host can be interpreted with a simple bonding model. We denote the combination of the host and impurity states coupled for the matrix element W as $\varphi_V^{(W)}$ and $\varphi_I^{(W)}$, and with an energetic separation $\Delta^{(W)}$. The subscripts V and I refer to the main character of the bands: VB or IB. For simplicity we will assume that $\delta = W/\Delta^{(0)}$ is small, limiting us to a first order in δ, although the conclusions are completely general. When the interaction takes place, the initial states mix; $\varphi_V^{(W)} = \varphi_V^{(0)} - \delta\varphi_I^{(0)}$ and $\varphi_I^{(W)} = \delta\varphi_V^{(0)} + \varphi_I^{(0)}$. The final states have an energetic separation $\Delta^{(W)} = \Delta^{(0)}(1+2\delta^2)$. The $\varphi_V^{(W)}$ is principally a bonding orbital (lower energy), whereas $\varphi_I^{(W)}$ is an antibonding orbital (larger energy). If initially the occupation number of the impurity state without interaction is $n_I^{(0)}$, the occupation number of the impurity in $\varphi_I^{(W)}$ is $n_I^{(W)} = (1+\delta^2)^{-1} n_I^{(0)} \approx (1-\delta^2) n_I^{(0)}$, and in $\varphi_V^{(W)}$ is $n_V^{(W)} = \delta^2(1+\delta^2)^{-1} n_I^{(0)} \approx \delta^2 n_I^{(0)}$. Therefore, a larger occupation of $\varphi_I^{(W)}$ (lower occupation of $\varphi_V^{(W)}$) is equivalent to a decrease in δ. In our context δ is the impurity–host interaction. A decrease in δ corresponds to an increment in Q. The bonding orbital $\varphi_V^{(W)}$ is more localized on the impurity site. Therefore, an increase in the occupation or a decrease in the impurity–host interaction, i.e., lower oc-

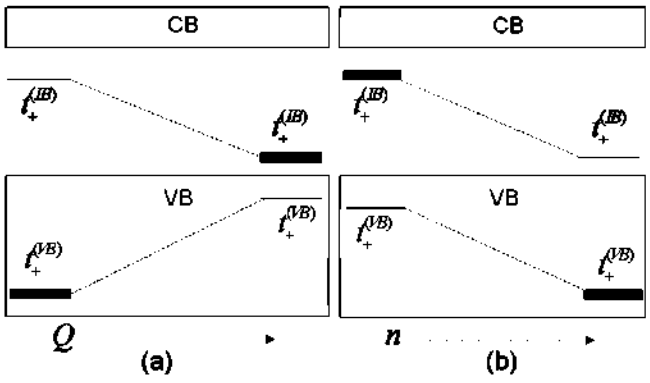

FIG. 5. (Color online) Schematic representation of the evolution of the $t_+^{(VB)}$ and $t_+^{(IB)}$ Cr states with Q (a) and n (b). The thick line indicates the largest contribution from these states to the VB or to the CB.

cupation of $\varphi_V^{(W)}$, to lead to a flow of electrons from impurity to host, and the impurity site remained essentially neutral.

This behavior is represented schematically in Fig. 5. This figure shows the qualitative behavior of Fig. 4. The change in Q or in the IB charge gives rise to, as consequence, a change in the contribution of the Cr atom to the VB and IB in such way that the Cr charge is almost constant. When Q or the IB population increases (n decreases) the contribution of the t_+-Cr states to the VB ($t_+^{(VB)}$) decreases and the contribution to the IB ($t_+^{(IB)}$) increases. If $t_+^{(VB)}$ decreases, there is an increment in the host contribution to the VB. Therefore, there is a flow of electrons from impurity to host.

This phenomenon is particular to impurities where the interaction impurity–host leads to the existence of impurity contributions to the IB and to the VB. It permits the stabilization of the density charge around the impurity through the modification of the contribution from the impurity to the IB and to the VB. This mechanism does not exist in free atoms or in impurities in ionic solids. In this latter case, the changes in the charge density because of charge-transfer processes can only be stabilized by a massive relaxation of the impurity via MPE. This has an obvious implication on the nature of the NRR. For the case of a system with an IB the equilibrium positions for different charges from the IB are very similar and the Huang–Rhys factor or the Frank–Condon shift will be small. It could decrease the NRR via MPE with respect to deep gap levels in other systems. Of course, other NRR mechanisms can be present. The stabilization of the density charge around the Cr in $Zn_{1-x}Cr_xS$ implies that the position of the minimums in Fig. 1 will be very similar, as is observed in Fig. 4. The crossing points Q_C and Q_V in Fig. 3, will be at very high energies. It will impede the capture processes within the MPE mechanism of the NRR.

An increase in the concentration of the impurity leads to the decrease in the NRR via MPE.[5] The reasons for this decrease are related to the Mott transition. In this case, the charges in the impurities are balanced by redistribution with the remaining impurities. From our results in this work, as well as the impurity–impurity interactions for large concentration,[5] there is another way of reducing the NRR as follows:[16] an increase in the impurity–host interaction. In this case, the equilibrium of the electronic density around the impurity is due to the modification of the contribution from the impurity to the IB and to the VB, i.e., a Le Chatelier principle.

V. CONCLUSIONS

We have carried out first-principles calculations for a Cr impurity in ZnS, and have analyzed the Cr–host interactions as a function of several configuration coordinates and the IB charge. The IB in these systems is the antibonding combination (larger energy) formed by the interaction of the Cr orbitals with the S orbitals. The bonding combination (lower energy) lies in the VB. For a different occupation of this IB, the charge around the impurity is balanced by the modification of the contribution from the impurity to the IB and to the VB. Consequently, there is a small variation in the equilibrium configurations and in the electronic density (and forces) around the Cr. This mechanism for balancing the charge between the impurities and the host semiconductor is additional to that resulting from the increment in the concentration of impurities.

Therefore, from these results, free carriers can be created by photons with energies lower than the host semiconductor band gap. The IB within these host semiconductors helps to increase the radiative transition rate with respect to the nonradiative decay rate via MPE, thus improving the emission quantum yield, in accordance with experimental results.

ACKNOWLEDGMENTS

This work has been supported by the GENESIS FV project of the National Spanish Program CONSOLIDER (Grant No. CSD2006-0004), by the European Commission through the funding of the project IBPOWER (Ref. No. Grant Agreement No. 211640), and by La Comunidad de Madrid through the funding of the project NUMANCIA-2 (Reference No. S-2009/ENE-1477).

[1] A. Luque and A. Martí, Phys. Rev. Lett. **78**, 5014 (1997).
[2] M. A. Luque, C. Stanley, N. Lopez, L. Cuadra, D. Zhou, J. L. Pearson, and A. McKee, J. Appl. Phys. **96**, 903 (2004); K. M. Yu, W. Walukiewicz, J. W. Ager III, D. Bour, R. Farshchi, O. D. Dubon, S. X. Li, I. D. Sharp, and E. E. Haller, Appl. Phys. Lett. **88**, 092110 (2006); W. Wang, A. S. Lin, and J. D. Phillips, *ibid.* **95**, 011103 (2009); S. Suraprapapich, S. Thainoi, S. Kanjanachuchai, and S. Panyakeow, Sol. Energy Mater. Sol. Cells **90**, 2968 (2006).
[3] C. H. Henry and D. V. Lang, Phys. Rev. B **15**, 989 (1977); D. V. Lang and C. H. Henry, Phys. Rev. Lett. **35**, 1525 (1975); K. V. Boer, *Survey of Semiconductor Physics* (Wiley, New York, 2002).
[4] C. Tablero, A. Martí, D. F. Marrón, E. Antolín, and A. Luque, Proceedings of the 23th European Photovoltaic Solar Energy Conference, Valencia, 2008.
[5] A. Luque, A. Martí, E. Antolín, and C. Tablero, Physica B **382**, 320 (2006).
[6] L. D. DeLoach, R. H. Page, G. D. Wilke, S. A. Payne, and W. F. Krupke, IEEE J. Quantum Electron. **32**, 885 (1996).
[7] C. Tablero, Comput. Mater. Sci. **37**, 483 (2006); Sol. Energy Mater. Sol. Cells **90**, 203 (2006); J. Chem. Phys. **123**, 114709 (2005); Phys. Rev. B **74**, 195203 (2006).
[8] J. M. Soler, E. Artacho, J. D. Gale, A. García, J. Junquera, P. Ordejon, and D. Sánchez-Portal, J. Phys.: Condens. Matter **14**, 2745 (2002), and references therein.
[9] J. E. Northrup and S. B. Zhang, Phys. Rev. B **47**, 6791 (1993).
[10] N. Troullier and J. L. Martins, Phys. Rev. B **43**, 1993 (1991); L. Kleinman and D. M. Bylander, Phys. Rev. Lett. **48**, 1425 (1982); D. M. Bylander and

L. Kleinman, Phys. Rev. B **41**, 907 (1990).
[11]O. F. Sankey and D. J. Niklewski, Phys. Rev. B **40**, 3979 (1989).
[12]D. M. Ceperley and B. J. Alder, Phys. Rev. Lett. **45**, 566 (1980).
[13]M. Godlewski and M. Kaminska, J. Phys. C **13**, 6537 (1980).
[14]J. Dieleman, R. S. Title, and W. V. Smith, Phys. Lett. **1**, 334 (1962); H. D. Fair, R. D. Ewing, and F. E. Williams, Phys. Rev. **144**, 298 (1966); K. Suto and M. Aoki, J. Phys. Soc. Jpn. **22**, 1121 (1967); T. Taki and H. Bo, *ibid.* **25**, 1324 (1968).
[15]D. M. Haldane and P. W. Anderson, Phys. Rev. B **13**, 2553 (1976).
[16]C. Tablero, Physica B **404**, 4023 (2009).